



# Analysis of constraining a chemical kinetic mechanism using hybrid response surface networks

Paxton Wiersema<sup>a,1</sup>, Ji-Hun Oh<sup>a,1</sup>, Keunsoo Kim<sup>a,b,1</sup>, Audrey Godsell<sup>a</sup>, Tonghun Lee<sup>a,\*</sup>

<sup>a</sup> University of Illinois Urbana-Champaign, Urbana, IL, United States of America

<sup>b</sup> Argonne National Laboratory, Lemont, IL, United States of America

## ARTICLE INFO

### Keywords:

Kinetic modeling  
Uncertainty quantification  
Response surface  
HyChem

## ABSTRACT

This paper presents an artificial intelligence based analysis for fast development of jet fuel chemical kinetic mechanisms through optimal constraining of parameters. The need to generate chemical kinetic mechanisms rapidly with less uncertainty is a critical requirement to efficiently assess newly introduced sustainable aviation fuels. To overcome the under-constrained nature of the optimization process with readily available but limited data, a hybrid response surface technique was developed to rapidly repeat this fitting process and provide a distribution of solutions. Through this approach, not only can the uncertainties be quantified, but the distribution of solutions can also be used to identify additional data that can reduce those uncertainties. Since extensive experimental measurements can be costly, the ability to identify a limited set of additional data can be of great importance. In this study, we demonstrate this approach using a Jet-A chemical kinetic mechanism that was optimized towards new experimental ignition delay measurements using the hybrid response surface network approach. This mechanism is shown to produce well-constrained ignition delay predictions at conditions of other ignition delay data in the literature, but significant uncertainty in chemical species were observed when compared to shock tube pyrolysis species measurements. By constraining one key chemical species from the response surface analysis, it is shown that most of the uncertainty in the remaining species was also reduced and utilizing two species provided extremely strong constraints. The results suggest that adding even a single species measurement to the mechanism development would significantly reduce the uncertainties in the optimization process.

## 1. Introduction

The development of practical chemical kinetic mechanisms for combustion simulations is an important task for the efficient and inexpensive testing and screening processes of new fuels. Considering recent attention on the environmental and economic concerns associated with the use of petroleum-based fuels, new sustainable aviation fuels are being created at an increasingly fast rate, but generating chemical kinetic models at the same speed is challenging. These sustainable aviation fuels can come from a wide variety of feed stocks and formulation processes which results in fuels with widely varying chemical compositions and combustion characteristics [1]. If a fuel is composed of a small number of well-known species, detailed modeling of the true chemical reactions may be possible, but these fuels are often composed of many species that cannot be fully modeled without extensive characterization of the fuel composition and extremely large chemical kinetic mechanisms [2]. These large mechanisms are not

practical for the realistic combustion simulations required for resolving the wide-ranging combustion characteristics of sustainable fuels [3].

Optimization methods have been used extensively in the past for the fitting of reaction models, most notably with Gri-Mech, but the uncertainty spaces of more recent models have continued to increase [4,5]. Numerous kinetic systems contain parameters that exhibit pronounced nonlinearities and couplings which lead to nonconvex optimization, implying that the optimized rate represents just one specific instance within a multi-modal distribution. The uncertainty of a chemical kinetic model arises from two factors: the simplicity of the model and the optimization process.

With the goal of rapidly developing mechanisms for new fuels, a data-driven optimization method was presented in previous works [6,7]. The optimized mechanisms accurately described conditions specified in the experimental target data, but the uncertainty in other parameters of the model could not be clearly identified. To better

\* Corresponding author.

E-mail address: [tonghun@illinois.edu](mailto:tonghun@illinois.edu) (T. Lee).

<sup>1</sup> These authors contributed equally to this work.

understand this problem, a hybrid response surface network technique was developed to search the uncertainty space in this data driven optimization process [8]. To adequately quantify these larger uncertainty spaces, deep learning based response surface approaches can bypass the large computational costs associated with this process [9,10]. The hybrid response surface network approach focuses on specific regions of interest since generating a general response surface can struggle to accurately approximate complex models with a high number of uncertain parameters through both high- and low-temperature chemistry.

This study presents a demonstration of the hybrid response surface network method using new experimental ignition delay measurements, thereby visually showing the uncertainty of an optimized mechanism through simulations of ignition delay and species measurements. In this study, Jet-A was chosen as the representative fuel due to its widespread use and abundant data, and a framework was developed for analysis. This abundant data can then be leveraged to show the constraining ability of additional validation data on the final model uncertainty. While ignition delay measurements are widely used for model validation, the information gained from this Jet-A constraining can be used to inform which other experimental measurements reduce the model uncertainties in the most efficient manner.

## 2. Experimental methods

Experimental ignition delay measurements have been the basis for the optimization of mechanisms using the data-driven and hybrid response surface network methods. Ignition delay offers key insights into the overall timescales of combustion which is critical for modeling because the design of many real combustors depends strongly on the chemical ignition timing of the fuel [11]. The accessibility of the experimental methods also allows for wide ranges of temperature, pressure, and equivalence ratio conditions to be measured. For this study, Jet-A was chosen as the fuel because of its standardized use in aviation and the availability of extensive experimental data. Jet-A is a petroleum derived aviation fuel with a broad distribution of components. The Jet-A used in this study is designated as A2 or POSF10325 by the National Jet Fuel Combustion Program [12].

To measure ignition delay, the shock tube at the University of Illinois Urbana-Champaign was used. This shock tube produces the test conditions through an incident and reflected shock in a heated driven section. The non-heated driver section of the shock tube is separated from the driven section by a expendable diaphragm with assisted bursting by a bladed insert to create consistent conditions between experiments and limit debris. A conical insert in the end of the driver section counteracts the test section pressure rise after the reflected shock. Measurement of the incident shock speed is taken from five evenly spaced PCB Piezotronics 113B22 pressure transducers while the ignition delay measurement was collected from an additional Kistler 603B pressure transducer near the end wall of the shock tube. Fuel mixtures, created from undiluted UN1002 air and evaporated liquid Jet-A, are prepared in an external heated mixing vessel that is fed into the shock tube through heated lines.

For mechanism development experimental target data, two pressures of 20 and 32.5 bar were chosen to validate conditions close to practical combustor systems and provide information on the pressure dependence of Jet-A. A temperature range from 650–1250 K was measured to cover high temperature, low temperature and negative temperature coefficient (NTC) chemistry regions. Equivalence ratios of 0.5, 1.0, and 1.3 were measured to represent fuel-lean, stoichiometric, and fuel-rich combustion respectively. A fuel-rich condition at 32.5 bar was not measured to limit soot deposition in the shock tube. The experimental ignition delay measurements for Jet-A are shown in Fig. 1 where the trends of low-temperature, NTC, and high-temperature ignition can be seen. In this study, simulations of ignition delay were performed in an ideal reactor without changes in temperature and pressure due to the pressure consistency seen in the test section during

**Table 1**

Fuel decomposition reaction set: HyChem Jet-A reactions unbolded, added reactions bolded (Jet-A: averaged fuel molecule, R: pseudo alkyl radical of Jet-A, Q: pseudo -2H molecule of Jet-A).

R1	Jet-A → (pyrolysis products)
R2	Jet-A + H → (R) + H <sub>2</sub>
R3	Jet-A + CH <sub>3</sub> → (R) + CH <sub>4</sub>
R4	Jet-A + OH → (R) + H <sub>2</sub> O
R5	Jet-A + O <sub>2</sub> → (R) + HO <sub>2</sub>
R6	Jet-A + HO <sub>2</sub> → (R) + H <sub>2</sub> O <sub>2</sub>
R7	Jet-A + O → (R) + OH
R8	(R) → (pyrolysis products)
R9	(R) + O <sub>2</sub> → (ROO)
R10	(ROO) ↔ (Q) + HO <sub>2</sub>
R11	(ROOH) ↔ (ROO) + OH
R12	(RO) → (pyrolysis products)
R13	(ROO) + HO <sub>2</sub> ↔ (ROOH) + O <sub>2</sub>
R14	(ROO) ↔ (QOOH)
R15	(QOOH) ↔ (QO) + OH
R16	(QO) → (pyrolysis products)
R17	(QOOH) ↔ HO <sub>2</sub> + (Q)
R18	(QOOH) + O <sub>2</sub> ↔ (OOQOOH)
R19	(OOQOOH) ↔ (HOOQ <sub>H</sub> O) + OH
R20	(HOOQ <sub>H</sub> O) → (pyrolysis products)
R21	(Q) → (pyrolysis products)

experimentation. Any tests with significant pressure changes due to contact surface, boundary layer, or early expansion interaction were disregarded. The simulation results of HRSN-SGDE in Fig. 1 will be explained in Section 4.

## 3. Chemical kinetic model

To rapidly develop a chemical kinetic mechanism for a multi-component jet fuel, it would be difficult to accurately model every major component in the mixture. The surrogate fuel modeling method circumvents this process by approximating the multi-component fuel as a mixture of well-known and previously modeled fuel species [13]. Another way of approximating the complicated fuel molecule is the HyChem method which approximates the multi-component fuel as a single averaged species and then lumps the fuel pyrolysis and oxidation reactions into a few reaction steps that terminate into smaller intermediate species [14]. The oxidation of these smaller intermediate species is described with a well validated detailed chemistry model (USC-Mech II) [15]. To reduce computational costs and allow for applicability to CFD, this study applied the HyChem Jet-A mechanism [14]. However, the framework developed in this study is versatile enough to accommodate other mechanisms, including reduced mechanisms. This Jet-A HyChem mechanism, with some modifications, is used as a case study to show the constraining ability of the hybrid response surface network when combined with strong experimental data.

The experimental temperature range covers much of the low temperature chemistry and NTC regions of the fuel. To leverage this data and provide additional uncertain values for this study, the low temperature chemistry sub-model in the HyChem Jet-A mechanism was modified to include additional reactions. The final set of the reactions in both the high temperature and low temperature sub-models are shown in Table 1, with the new reactions shown in bold. The structure of the low temperature chemistry sub-model is taken from the work on low temperature chemistry by Zádor et al. [16]. The changes add additional pathways for the decomposition of the alkylperoxy radical (ROO) and the hydroperoxyalkyl radical (QOOH).

## 4. Hybrid response surface network

With experimental ignition delay measurements and the base Jet-A mechanism, the reaction rate coefficient fitting procedure could be completed. The reactions shown in Table 1 are the variable reactions

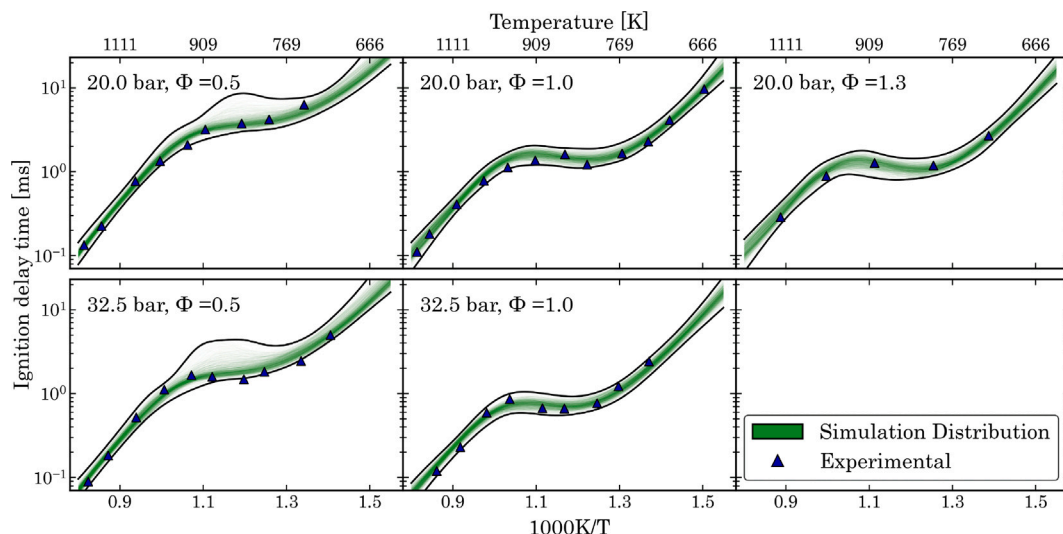


Fig. 1. Experimental (symbols) ignition delay of Jet-A and constrained simulations (lines: actual simulations in green with upper and lower bounds in black) from HRSN-SGDE at pressures of 20, and 32.5 bar and equivalence ratios of  $\phi = 0.5, 1.0,$  and  $1.3$ .

for the optimization with unchanged nominal reaction rate coefficients from the Jet-A HyChem mechanism. Nominal reaction rate coefficients for the new low-temperature pathways were selected from similar reactions in literature. All Arrhenius reaction rate coefficients, referenced as the pre-exponential factor ( $A$ ), temperature dependence coefficient ( $n$ ), and activation energy ( $E_a$ ), were allowed to be modified, other than those that were nominally zero. The temperature dependence coefficients in the reactions for the low-temperature chemistry sub-model are all set equal to zero [17]. The two activation energies for Reaction 9 (R9) and Reaction 18 (R18) were also set to zero, which are reactions with  $O_2$  in the low temperature sub-model as described by the HyChem Jet-A mechanism [14]. The parameter boundaries were selected from the molecules of the highest and lowest chemical reactivities from the Jet-A composition [12]. Roughly, bounds of  $\pm 2$  for log of  $A$ ,  $\pm 2$  for  $n$ ,  $\pm 30\%$  for  $E_a$  were chosen.

While the optimization method can provide reliable fits of experimental target data, which in this study is ignition delay, it does not guarantee a globally optimal solution or provide information about possible other solutions. These uncertainties are critical for evaluating a mechanism and can be quantified by repeating the optimization process many times. Because a single optimization requires significant computational cost, the time cost of this repetition scales rapidly to an infeasible amount even with extensive computational capabilities. To solve this problem, the hybrid response surface network and stochastic gradient descent ensemble (HRSN-SGDE) technique was developed to significantly decrease the time needed to run the optimizations. The introductory work on this technique demonstrated the benefits and structure of the method in detail and a summary is presented here [8].

#### 4.1. Model overview

The HRSN model in the context of this study can be generally described as a method to approximate the simulation of ignition delays from an input of reaction rate coefficients. This allows this model to be directly substituted for the true and expensive simulation in the mechanism optimization process. This model is not general to all possible reaction rate coefficients and any temperature, pressure, and equivalence ratio condition. Instead, it must be trained for specific coefficients that are bound to a finite range and for a defined set of output ignition delay conditions.

Due to the large simulation space that is being approximated by this model, it was not possible to efficiently create a response surface model that accurately fit this entire space. To solve this issue, a two

model approach was developed instead. The first model, called the local surrogate, is trained only on data from a reduced sub-space which produces simulation results near to the target experimental data. Because the local surrogate is trained on a reduced data space, it is much more accurate for this important region of data. The second model, called the classifier, generally predicts how likely a random sample is to be in this reduced target sub-space. The full HRSN-SGDE process is split into random sampling, active sampling, and solution generation steps, where the first two steps train the local surrogate and classifier models, and the final step applies these models to rapidly optimize the Jet-A mechanism.

#### 4.2. Model training

To create the models, a large set of training data is needed to adequately covers the search space. This study applied sobol sampling, which is a quasi-random selection process to more efficiently cover the search space. For the number of inputs parameters and output conditions, an optimal sampling size was found to be on the order of one million. After random sampling, the local surrogate and classifier models can be trained. Samples within the reduced target sub-space, defined as  $\pm 0.5$  around the log normalized target ignition delay values, are used to train the local surrogate, while the classifier is trained on the full data set. The probabilistic structure of these two models can then inform future sampling so that it focuses on regions where the models have inaccuracies. This process, called active sampling, prioritizes regions first that the classifier predicts to be within the target sub-space and the local surrogate is uncertain, and second where the classifier itself is uncertain. Active sampling and model training in batches improves the accuracy of the two models at a much faster rate than further random sampling and is terminated once both the local surrogate and classifier accuracy is at a sufficient level. Some error is allowed to limit the time required for training.

#### 4.3. Solution generation

With trained local surrogate and classifier models, the optimization process can be completed without costly simulations. A benefit of the HRSN method is that the resulting models are differentiable, and the optimization problem can be completed using stochastic gradient descent (SGD). The classifier imposes a strong gradient towards the target sub-space where the local surrogate then controls the output more precisely and the SGD can converge to a solution. Maximum error

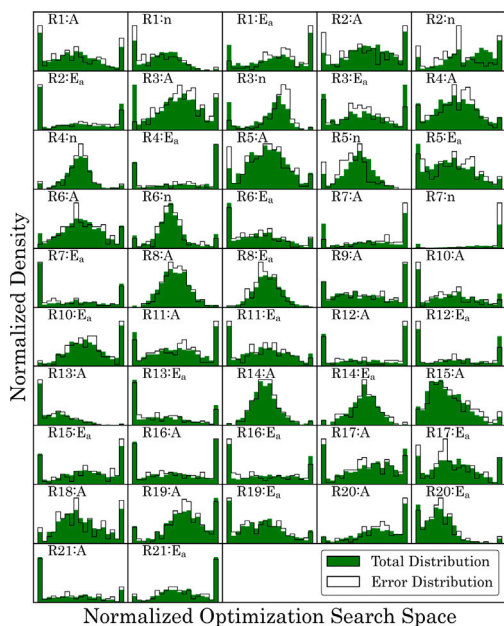


Fig. 2. Histogram of each modified reaction rate coefficient for the full solution set and solution set with simulation numerical error.

bounds are imposed on the final solution so that non-optimal solutions are screened. To create the distribution of solutions, the optimization process is repeated with varying initial reaction rate coefficients which were pulled randomly from a normal distribution inside the search space. Compared to pulling from a uniform distribution, the normal distribution slightly favored solutions towards the center of the distribution. With the wide uncertainty bounds chosen for this study, the normal distribution was preferred.

## 5. HRSN-SGDE results

### 5.1. Optimized parameter distributions

HRSN-SGDE was then applied to the Jet-A base mechanism to generate one thousand reaction models that were optimized towards the experimental ignition delay measurements. The random sampling process consisted of one million samples before transitioning to active sampling with five-hundred thousand samples. The distributions of the solution reaction rate coefficients are shown in Fig. 2. A notable feature of the rate coefficient histograms are the large tails that appear at the boundaries of the search space. This is an artifact of the optimization process and indicates that for many of the solutions, the ideal location of a parameter likely occurred outside of the set boundaries. While this artifact is not ideal, completely unbounded optimizations are not physical, so the chosen boundaries will necessarily have some effect on the final solution set. The non-ideal solution also produced ignition delays within the error limit of the optimization, which indicates that any improvements from moving outside of the set boundaries are negligible since all solutions within the error limit are considered to be of equal value.

When simulating results that will be shown in future sections, a portion of the mechanisms occasionally triggered numerical errors that caused the simulations to fail. The mechanisms where these errors occur are shown alongside the full solution histogram. Many of the error distributions appear nearly identical to the full distributions, indicating that those parameters were likely not the cause of the numerical errors. The temperature power coefficients (n) contribute significantly to the appearance of an error, particularly in reaction seven (R7). When choosing a final mechanism, regions with a high error probability should be avoided.

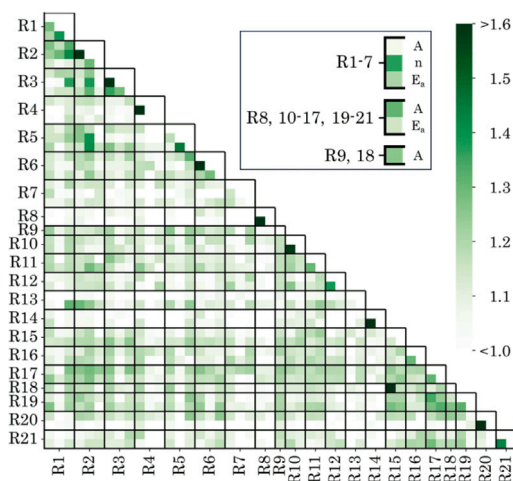


Fig. 3. Relative magnitude of correlation between each of the reaction rate coefficients that are modified in this study.

### 5.2. Reaction rate coefficient correlations

To further study the solution space of the reaction rate coefficients, the joint correlations between each optimized coefficient are shown in Fig. 3. As expected, the largest correlations are found between the coefficients of the same reaction. The scaling of the heat map was adjusted to amplify any variation between reactions rather than focusing on intra-reaction outliers, but even with this amplification, very few correlations are notable. The largest inter-reaction correlation occurs between “R18:A” and “R15:A”. Additionally, the correlations between high-temperature coefficient reactions one through five, and the correlations between low-temperature coefficient reactions fifteen through nineteen are more distinct as groups. Overall, the lack of strong and distinct correlations between the optimized reaction rate coefficients suggests that the optimization convergence is not dependent on only a small set of reactions and rather is dependent on a more complex combination of the full set of reactions.

The joint probability density functions (PDF) of these two regions are shown in more detail with the selected high-temperature coefficients in Fig. 4(a) and the low-temperature coefficients in Fig. 4(b). By comparing the actual joint distribution of solutions to an uncorrelated joint distribution, any differences show rate coefficient coupling during the optimization. A large shift of the actual distribution from the uncorrelated distribution indicates that the relationship between those reaction rate coefficients were important to the final converged solutions. The high temperature coefficient PDFs clearly show the strong intra-reaction correlation of Reaction 5 with a nearly linear solution distribution compared to the round uncorrelated distribution. The remaining high-temperature correlations show some deviation from the uncorrelated baseline, such as “R5:E<sub>a</sub>” with “R2:n” where the peaks of the distribution are slightly shifted.

The “R18:A” and “R15:A” joint PDF shows a strong correlation. The competition between these two reactions determines the balance of final pyrolysis pathways in the low-temperature sub-model of the mechanism. Reaction 15 defines QOOH to QO conversion, which is followed by the QO pyrolysis reaction. These reactions result in the generation of OH radicals at lower temperatures, subsequently leading to the production of water and heat. This increase in temperature diminishes the time delay for the fuel to reach the decomposition temperature of H<sub>2</sub>O<sub>2</sub>. Reaction 18 converts QOOH to OOQOOH which has the possible pyrolysis pathways of Q and HOOQ<sub>H</sub>O. The QOOH to QO pathway was one of the additions to the original HyChem Jet-A mechanism and the strong correlation between these rate coefficients suggests that the balance of these two reaction rates in this version

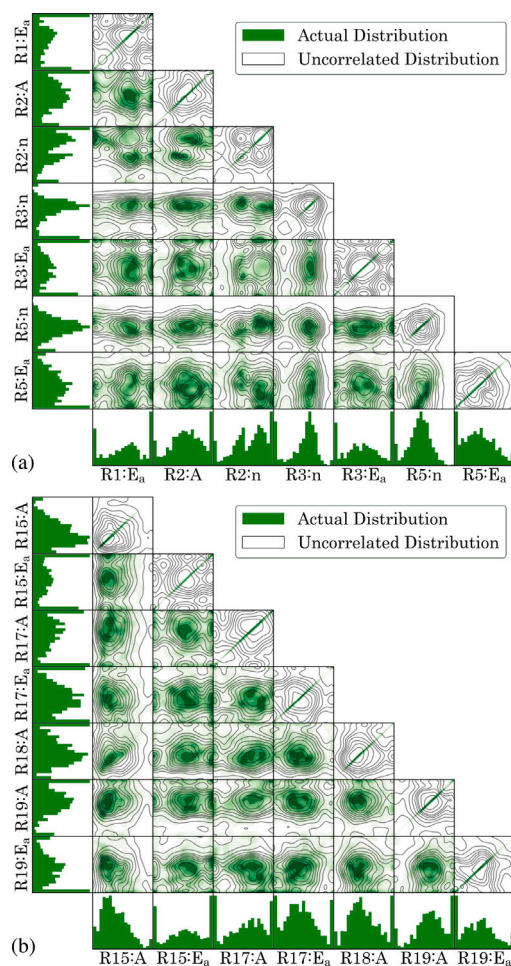


Fig. 4. Selected joint PDFs of high (a) and low (b) temperature sub-model reaction rate parameters.

of the mechanism is important to the low-temperature ignition delay times. This correlation is not unexpected as this balance between the chain branching initiated by the addition of  $O_2$  to QOOH and the decomposition of QOOH has been shown to be critical in other works [18]. The remaining low temperature joint PDFs are similar to the high-temperature correlations, with slightly shifted distributions but no significant trends.

### 5.3. Fitting of experimental conditions

The ignition delays simulated from the optimized chemical kinetic mechanisms of Jet-A are shown with the experimental ignition delays in Fig. 1. Because of the error limit defined in the optimization process, the mechanisms are well constrained at these conditions. The fuel-lean high pressure condition exhibits the most error at intermediate temperatures, as the NTC behavior is not matched perfectly. At the fuel-lean conditions, there is a small subset of mechanisms that have significantly larger error than the average which is likely caused by an imperfect HRSN model and can be screened out when choosing a final mechanism.

## 6. Mechanism validation and constraining

### 6.1. Ignition delay

To better understand the constraining ability of additional ignition delay measurements and the applicable range of the mechanisms optimized by the response surface and gradient descent, Jet-A (POSF10325)

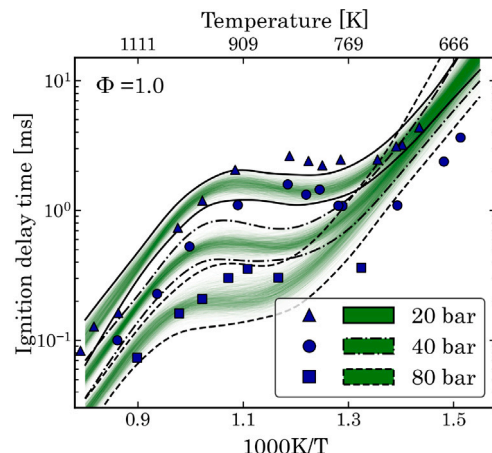


Fig. 5. Ignition delay simulation distributions (lines) and experimental data (symbols) from Burden et al. [19] at 20, 40, and 80 bar and  $\phi = 1.0$ .

experimental ignition delays were referenced from Burden et al. at Rensselaer Polytechnic Institute (RPI) [19]. The experimental measurements cover pressures of 20, 40 and 80 bar with stoichiometric fuel and air mixtures as shown in Fig. 5. At the 20 bar condition the RPI experimental data agrees with the new experimental data measured in this study at high temperatures, above 900 K, and at the lowest temperatures, below 750 K, but was measured to have longer ignition delays in the NTC region. When comparing the RPI experimental data to the distribution of optimized mechanisms at the higher pressure conditions not measured in this study, more error is found. At the 40 bar condition, more significant error is seen in the NTC region and large error occurs at the lowest temperatures, but the high temperature data matches well with the simulations. The 80 bar condition has a similar trend to 40 bar but the error in the NTC is smaller.

The experimental ignition delay disagreement between this study and RPI at 20 bar and temperatures between 750 and 900 K appears to be propagated through the higher pressure conditions. While the fuels in both studies are ostensibly the same, low-temperature ignition behavior is sensitive and any batch differences between studies could have a significant effect. Even though there is error between the simulations and the experimental data, the simulation distribution itself is already well constrained at the 40 bar condition and only very high pressure measurements would add any significant constraint to the solution space.

### 6.2. Pyrolysis species measurements

The versatility of the constrained model was tested through application to shock tube pyrolysis species data of Jet-A taken at the University of Illinois Chicago [20]. The pyrolysis experimental data includes the concentrations of twelve intermediate species in the breakdown of Jet-A over a range of temperatures for pressure conditions of 25 and 90 atm. The 25 atm pressure case was used for this study. This experimental data is contrasted with the species concentrations obtained from usage of the one thousand optimized mechanisms in the “Unconstrained” columns in Fig. 6. The mechanisms qualitatively show good agreement with the pyrolysis data for some species, and poor agreement for other species. Often, the mechanisms produce distinct modes where groups of mechanisms agree for a species across the temperature range.

A quantitative metric known as mean absolute percentage error (MAPE) assesses the error between each mechanism’s species prediction and the experimental data. MAPE is computed separately for each species and optimized mechanism at each experimental temperature condition including those where the experimental value is near zero.

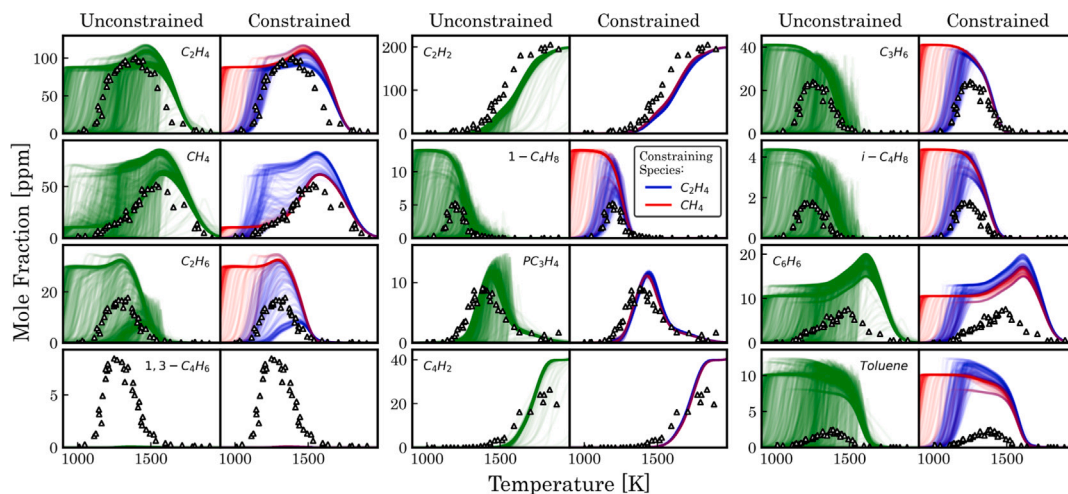


Fig. 6. Unconstrained and constrained distribution of Jet-A pyrolysis species simulations (lines) compared to experimental measurements (symbols) from Han et al. [20].

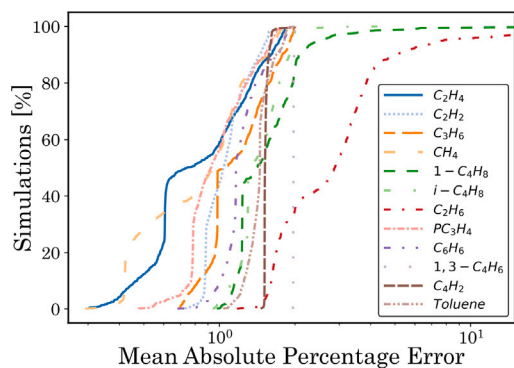


Fig. 7. Error of simulation to experimental pyrolysis data for each species.

While these zero regions do create a larger error, this prioritizes simulations that match the temperature trend of the experimental results. Results in Fig. 7 show, for each of the 12 species, the percentage of optimized models that produce simulations with an error below the value on the x-axis. Larger error values correspond to concentration profiles with larger deviations from the experimental data. All 100% of the mechanisms for a given species are included when the maximal error for that species is reached.

A vertical line in Fig. 7 indicates a region where many mechanism profiles produce the same error from the experimental data. The step-like behavior of some species, such as ethylene ( $C_2H_4$ ), exhibits the presence of multiple distinct modes in the mechanism predictions. The MAPE metric suggests an ideal species to constrain the mechanisms would be a species with low error from the experimental data as well as step-like behavior allowing the elimination of as many larger-error mechanisms as possible. The “Constrained” column in Fig. 6 shows the effects of constraining the one thousand mechanisms by the species  $C_2H_4$  and methane ( $CH_4$ ), the two species with the lowest error values.

Each of the two constraining species pares the mechanism set of one thousand down to the 15% of solutions with the lowest error with respect to the constraining species.  $C_2H_4$  and  $CH_4$  constrain some species similarly, such as diacetylene ( $C_4H_2$ ). Other species, such as propene ( $C_3H_6$ ), show little overlap in the remaining mechanisms left by the two constraining species. While using an individual species as a constraining tool can significantly reduce the uncertainty space of the optimization problem, combining as a joint species constraint is even more effective. The resulting constrained space is reduced to 1.8% of the original size when combining the two species with 15% constrained

spaces. This indicates that the  $C_2H_4$  and  $CH_4$  species histories have very low correlation and are an especially effective combination for constraining this Jet-A mechanism. Each of the two constraining species pares the mechanism set of one thousand down to the 15% of solutions with the lowest error with respect to the constraining species.  $C_2H_4$  and  $CH_4$  constrain some species similarly, such as diacetylene ( $C_4H_2$ ). Other species, such as propene ( $C_3H_6$ ), show little overlap in the remaining mechanisms left by the two constraining species. While using an individual species as a constraining tool can significantly reduce the uncertainty space of the optimization problem, combining as a joint species constraint is even more effective. The resulting constrained space is reduced to 1.8% of the original size when combining the two species with 15% constrained spaces. This indicates that the  $C_2H_4$  and  $CH_4$  species histories have very low correlation and are an especially effective combination for constraining this Jet-A mechanism.

## 7. Application beyond Jet-A

While the method shown in this work was demonstrated on Jet-A, the future application would be the development of mechanisms for SAFs to predict their performance in existing and future combustion systems. This method requires both a base mechanism structure that can represent the SAF composition as well as experimental data. The compositions of some sustainable fuels would be inadequately represented by the HyChem based model structure presented here, though this model formulation can be adapted for SAFs as has been done for an alcohol-to-jet fuel [21]. For fuels with oxygenated compounds, a modified HyChem structure that separately models the oxygenated and non-oxygenated compounds could be applied, as has been done with gasoline and ethanol mixtures [22]. If this is still insufficient, a surrogate fuel mechanism can also be optimized using the HRSN-SGDE method presented in this work by identifying uncertain reaction rates or optimizing the surrogate fuel fractions [23]. Significant experimental data sets for SAFs have already been collected in works such as those by Oßwald et al. and Kathrotia et al. [24,25]. While it was shown here that benzene ( $C_6H_6$ ) and toluene were constrained by  $C_2H_4$  and  $CH_4$ , the HyChem approach does not model all possible soot precursors and care should be taken in future mechanisms to validate soot precursors with experiments like those just referenced. For newer fuels without experimental testing, a reduced set of experimental data should be collected that prioritizes key performance conditions and species for a specific application to minimize development time.

## 8. Conclusion

Using the hybrid response surface networks followed by stochastic gradient descent ensemble method, one thousand mechanisms were optimized towards new experimental ignition delay measurements of Jet-A. Analysis of the resulting distribution showed that the current experimental ignition delay measurements were sufficient to constrain the ignition delays of the mechanism, but species histories showed unconstrained behavior. By utilizing species data from literature, it was shown that even a single species can constrain the solution space well, but two species when chosen correctly can significantly decrease the uncertainty in the mechanism. The authors want to highlight that while this paper delves into a jet fuel mechanism using the HyChem approach, the suggested framework is adaptable to virtually all kinetic models. The methodology employed in this research facilitates the swift generation of mechanisms for newly introduced sustainable aviation fuels.

## Novelty and significance statement

The result of the current work presents a method to rapidly generate chemical kinetic mechanisms and identify the most efficient way to reduce the uncertainty through the use of a machine learning based hybrid response surface approach. Such a process is an urgent need for sustainable aviation fuels as they are being created at an increasing rate. This work is significant as it visually shows how additional experimental measurements can impact the ability to constrain the mechanism and reduce the uncertainty. Without the machine learning approach, uncertainty quantification would be prohibitively costly in terms of computational time. As a result, the novel methodology proposed here allows for the creation of mechanisms that are reliable, computationally efficient, and able to be developed with a limited set of validation data.

## CRedit authorship contribution statement

**Paxton Wiersema:** Investigation, Data collection, Data analysis, Writing – original draft. **Ji-Hun Oh:** Response surface design, Writing-review. **Keunsoo Kim:** Conceptualization, Investigation, Writing-review. **Audrey Godsell:** Data analysis, Writing – original draft. **Tonghun Lee:** Research oversight, Writing-review.

## Declaration of competing interest

The authors declare that they have no known competing financial interests or personal relationships that could have appeared to influence the work reported in this paper.

## Acknowledgments

Support was provided by the US Federal Aviation Administration (FAA) Office of Environment and Energy as a part of ASCENT Project 33 under FAA Award Number: 13-C-AJFE-UI Amendment 33. Any opinions, findings, and conclusions or recommendations expressed in this material are those of the authors and do not necessarily reflect the views of the FAA or other ASCENT sponsors.

## Appendix A. Supplementary data

Supplementary material related to this article can be found online at <https://doi.org/10.1016/j.proci.2024.105522>.

## References

- [1] S.H. Won, J. Santner, F. Dryer, Y. Ju, Comparative evaluation of global combustion properties of alternative jet fuels, in: 51st AIAA Aerospace Sciences Meeting Including the New Horizons Forum and Aerospace Exposition, 2013, p. 156.
- [2] H.J. Curran, Developing detailed chemical kinetic mechanisms for fuel combustion, *Proc. Combust. Inst.* 37 (1) (2019) 57–81.
- [3] V. Burger, A. Yates, T. Mosbach, B. Gunasekaran, Fuel influence on targeted gas turbine combustion properties: Part II—detailed results, in: *Turbo Expo: Power for Land, Sea, and Air*, vol. 45653, American Society of Mechanical Engineers, 2014, V03AT03A003.
- [4] G.P. Smith, D.M. Golden, M. Frenklach, N.W. Moriarty, B. Eiteneer, M. Goldenberg, C.T. Bowman, R.K. Hanson, S. Song, et al., [http://www.me.berkeley.edu/gri\\_mech/](http://www.me.berkeley.edu/gri_mech/).
- [5] N. Sikalo, O. Hasemann, C. Schulz, A. Kempf, I. Wloka, A genetic algorithm-based method for the automatic reduction of reaction mechanisms, *Int. J. Chem. Kinet.* 46 (1) (2014) 41–59.
- [6] J.I. Ryu, K. Kim, K. Min, R. Scarcelli, S. Som, K.S. Kim, J.E. Temme, C.-B.M. Kweon, T. Lee, Data-driven chemical kinetic reaction mechanism for F-24 jet fuel ignition, *Fuel* 290 (2021) 119508.
- [7] K. Kim, P.W. Wiersema, J.I. Ryu, E. Mayhew, J. Temme, C.-B. Kweon, T. Lee, Data-driven approaches to optimize chemical kinetic models, in: *AIAA SCITECH 2022 Forum*, 2022.
- [8] J.-H. Oh, P. Wiersema, K. Kim, E. Mayhew, J. Temme, C.-B. Kweon, T. Lee, Fast uncertainty reduction of chemical kinetic models with complex spaces using hybrid response-surface networks, *Combust. Flame* 253 (2023) 112772.
- [9] K. Lin, Z. Zhou, C.K. Law, B. Yang, Dimensionality reduction for surrogate model construction for global sensitivity analysis: Comparison between active subspace and local sensitivity analysis, *Combust. Flame* 232 (2021) 111501.
- [10] D.A. Sheen, H. Wang, The method of uncertainty quantification and minimization using polynomial chaos expansions, *Combust. Flame* 158 (12) (2011) 2358–2374.
- [11] S.S. Vasu, D.F. Davidson, R.K. Hanson, Jet fuel ignition delay times: Shock tube experiments over wide conditions and surrogate model predictions, *Combust. Flame* 152 (1) (2008) 125–143.
- [12] M. Colket, J. Heyne, M. Rumizen, M. Gupta, T. Edwards, W.M. Roquemore, G. Andac, R. Boehm, et al., Overview of the national jet fuels combustion program, *AIAA J.* 55 (4) (2017) 1087–1104.
- [13] F.L. Dryer, S. Jahangirian, S. Dooley, S.H. Won, J. Heyne, V.R. Iyer, T.A. Litzinger, R.J. Santoro, Emulating the combustion behavior of real jet aviation fuels by surrogate mixtures of hydrocarbon fluid blends: Implications for science and engineering, *Energy Fuels* 28 (5) (2014) 3474–3485.
- [14] R. Xu, K. Wang, S. Banerjee, J. Shao, T. Parise, Y. Zhu, S. Wang, A. Movaghar, D.J. Lee, et al., A physics-based approach to modeling real-fuel combustion chemistry – II. Reaction kinetic models of jet and rocket fuels, *Combust. Flame* 193 (2018) 520–537.
- [15] H. Wang, X. You, A.V. Joshi, S.G. Davis, A. Laskin, F. Egolfopoulos, C.K. Law, USC mech version II. High-temperature combustion reaction model of H<sub>2</sub>/CO/C1-C4 compounds, 2007, [http://ignis.usc.edu/USC\\_Mech\\_II.htm](http://ignis.usc.edu/USC_Mech_II.htm).
- [16] J. Zádor, C.A. Taatjes, R.X. Fernandes, Kinetics of elementary reactions in low-temperature autoignition chemistry, *Prog. Energy Combust. Sci.* 37 (4) (2011) 371–421.
- [17] E. Ranzi, C. Cavallotti, A. Cuoci, A. Frassoldati, M. Pelucchi, T. Faravelli, New reaction classes in the kinetic modeling of low temperature oxidation of n-alkanes, *Combust. Flame* 162 (5) (2015) 1679–1691.
- [18] P. Zhao, C.K. Law, The role of global and detailed kinetics in the first-stage ignition delay in NTC-affected phenomena, *Combust. Flame* 160 (11) (2013) 2352–2358.
- [19] S. Burden, A. Tekawade, M.A. Oehlschlaeger, Ignition delay times for jet and diesel fuels: Constant volume spray and gas-phase shock tube measurements, *Fuel* 219 (2018) 312–319.
- [20] X. Han, M. Liszka, R. Xu, K. Brezinsky, H. Wang, A high pressure shock tube study of pyrolysis of real jet fuel Jet A, *Proc. Combust. Inst.* 37 (1) (2019) 189–196.
- [21] K. Wang, R. Xu, T. Parise, J. Shao, A. Movaghar, D.J. Lee, J.-W. Park, Y. Gao, T. Lu, et al., A physics-based approach to modeling real-fuel combustion chemistry – IV. HyChem modeling of combustion kinetics of a bio-derived jet fuel and its blends with a conventional Jet A, *Combust. Flame* 198 (2018) 477–489.
- [22] R. Xu, C. Saggese, R. Lawson, A. Movaghar, T. Parise, J. Shao, R. Choudhary, J.-W. Park, T. Lu, et al., A physics-based approach to modeling real-fuel combustion chemistry – VI. Predictive kinetic models of gasoline fuels, *Combust. Flame* 220 (2020) 475–487.
- [23] T. Kathrotia, P. Oßwald, C. Naumann, S. Richter, M. Köhler, Combustion kinetics of alternative jet fuels, part-II: Reaction model for fuel surrogate, *Fuel* 302 (2021) 120736.
- [24] P. Oßwald, J. Zinsmeister, T. Kathrotia, M. Alves-Fortunato, V. Burger, R. van der Westhuizen, C. Viljoen, K. Lehto, R. Sallinen, et al., Combustion kinetics of alternative jet fuels, Part-I: Experimental flow reactor study, *Fuel* 302 (2021) 120735.
- [25] T. Kathrotia, P. Oßwald, J. Zinsmeister, T. Methling, M. Köhler, Combustion kinetics of alternative jet fuels, part-III: Fuel modeling and surrogate strategy, *Fuel* 302 (2021) 120737.

## Technical Report Documentation Page

1. Report No.	2. Government Accession No.	3. Recipient's Catalog No.	
4. Title and Subtitle		5. Report Date	
		6. Performing Organization Code	
7. Author(s)		8. Performing Organization Report No.	
9. Performing Organization Name and Address		10. Work Unit No. (TRAIS)	
		11. Contract or Grant No.	
12. Sponsoring Agency Name and Address		13. Type of Report and Period Covered	
		14. Sponsoring Agency Code	
15. Supplementary Notes			
16. Abstract			
17. Key Words		18. Distribution Statement	
19. Security Classif. (of this report) <b>Unclassified</b>	20. Security Classif. (of this page) <b>Unclassified</b>	21. No. of Pages	22. Price